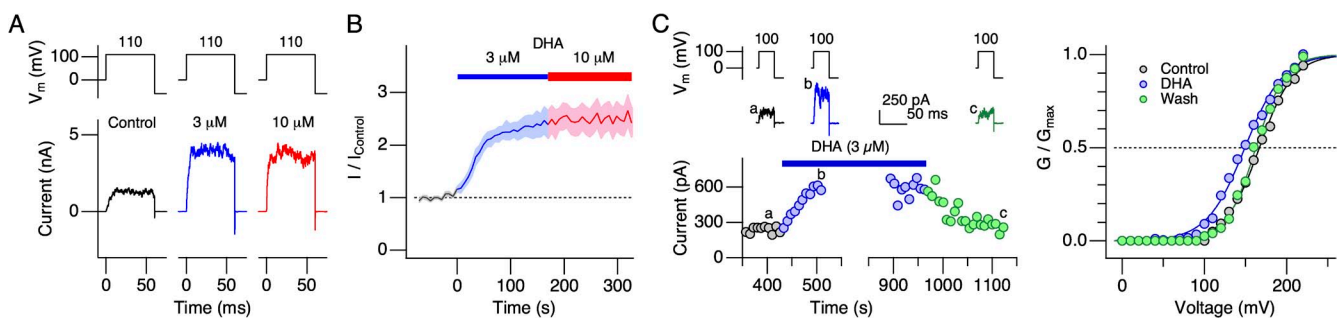
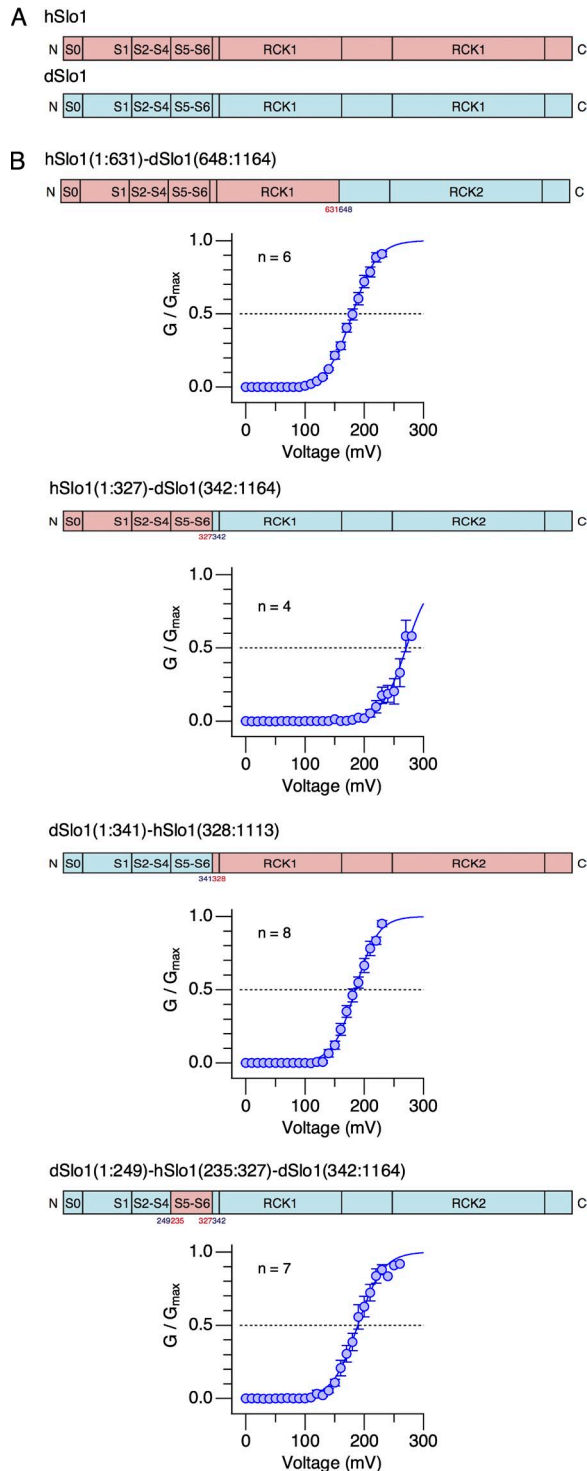
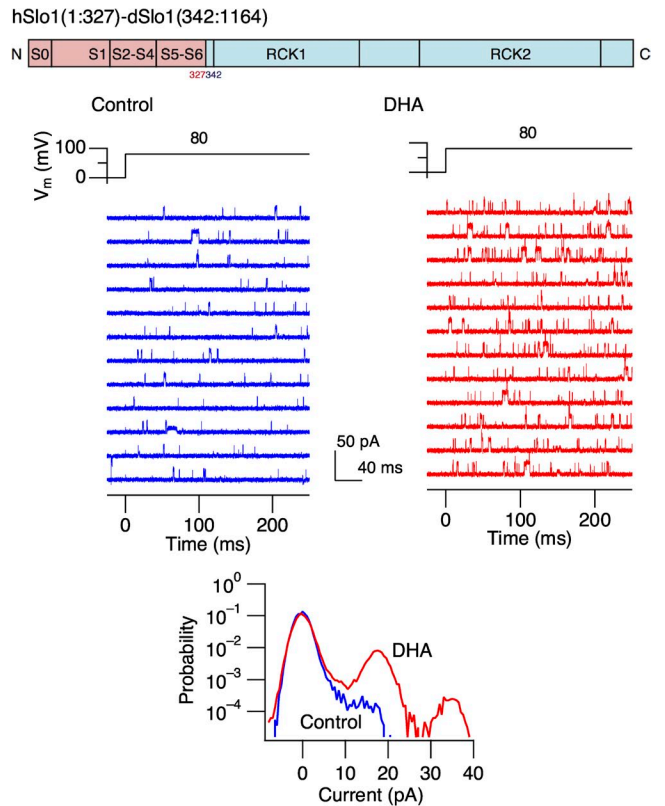


Hoshi et al., <http://www.jgp.org/cgi/content/full/jgp.201311061/DC1>

**Figure S1.** The concentration dependence and reversibility of the DHA action on the Slo1 channel without any auxiliary subunit. (A) The current-enhancing effect of DHA is saturated at  $\sim 3 \mu\text{M}$ . Representative currents at 110 mV before and after the application of 3 and 10  $\mu\text{M}$  DHA. (B) Mean peak outward current size at 110 mV as a function of time. Note that  $G/G_{\text{max}}$  is only  $\sim 0.15$  in the presence of 3  $\mu\text{M}$  DHA (see Fig. 1 C). The line width indicates SEM.  $n = 7$ . (C) Sample currents (left), peak outward currents (left), and G-V curves (right) recorded before the application of DHA (black), in the presence of 3  $\mu\text{M}$  DHA (blue) and after wash out of DHA (green). The patch was excised at  $t = 0$  s. The smooth curves in C (right) are Boltzmann fits to the results. Their  $V_{0.5}$  and  $Q_{\text{app}}$  values are  $166.9 \pm 1.1$  mV and  $1.21 \pm 0.06$ ,  $149.3 \pm 2.0$  mV and  $1.08 \pm 0.08$ , and  $162.7 \pm 1.1$  mV and  $1.39 \pm 0.07$  for the results before the application of DHA, in the presence of DHA, and after wash-out, respectively. Currents were recorded without  $\text{Ca}^{2+}$ .



**Figure S2.** Voltage dependence of activation of human-*Drosophila* chimeric Slo1 channels. (A) Schematic organizational diagrams of hSlo1 (pink) and dSlo1 (light blue). (B)  $G$ - $V$  curves of the chimeric channels indicated. The smooth curves represent Boltzmann fits to the results. From top to bottom, the  $V_{0.5}$  and  $Q_{app}$  values are  $180.0 \pm 0.9$  mV and  $1.18 \pm 0.05$ ,  $270.8 \pm 2.6$  mV and  $1.20 \pm 0.15$ ,  $185.0 \pm 1.5$  mV and  $1.31 \pm 0.09$ , and  $189.1 \pm 2.0$  mV and  $1.17 \pm 0.10$ .



**Figure S3.** DHA increases  $P_o$  in hSlo1(1:327)-dSlo1(342:1164). Representative openings before (blue, left) and after (red, right) the application of  $3 \mu\text{M}$  DHA in the absence of  $\text{Ca}^{2+}$ . Current responses to consecutive voltage pulses are shown. The normalized amplitude histogram below compares  $P_o$ .

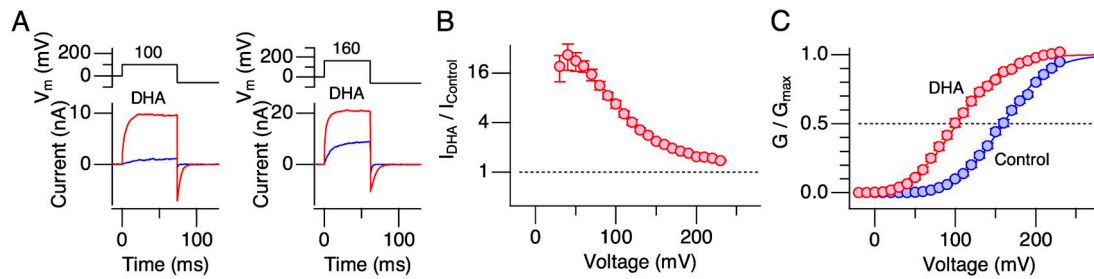


**Figure S4.** Enhancement of currents through wild-type hSlo1+h $\beta$ 1 channels by DHA in the absence of intracellular  $Ca^{2+}$ . (A) Representative currents before (blue) and after (red) the addition of DHA to the intracellular side at 100 mV ( $G/G_{max} = \sim 0.1$ ) and 160 mV ( $G/G_{max} = \sim 0.5$ ). (B) Fractional increases in peak outward currents at different voltages by DHA.  $n = 13$ . (C) G-V curves before (blue) and after (red) the application of DHA. The smooth curves represent Boltzmann fits to the data. The  $V_{0.5}$  and  $Q_{app}$  values are  $160.0 \pm 1.2$  mV and  $0.90 \pm 0.03$  for the control group and  $102.1 \pm 1.7$  mV and  $0.91 \pm 0.05$  for the DHA group.  $n = 13$ . DHA was applied at 3  $\mu$ M. The results include those reported in Hoshi et al. (2013. *Proc. Natl. Acad. Sci. USA*. 110:4816–4821) and additional measurements.

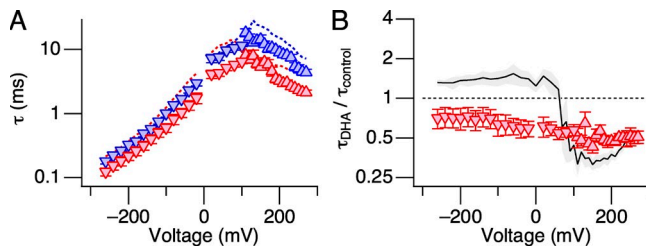


**Figure S5.** Effects of 3  $\mu$ M DHA on current kinetics of hSlo1 Y318S+h $\beta$ 1. (A) Voltage dependence of current relaxation time constant before (blue) and after (red) the application of DHA in hSlo1 Y318S+h $\beta$ 1. The average results obtained from wild-type hSlo1+h $\beta$ 1 are also shown using dashed traces (red, before DHA; blue, after DHA application). (B) Voltage dependence of fractional changes in the time constant of current relaxation in hSlo1 Y318S+h $\beta$ 1 (red) and wild-type hSlo1+h $\beta$ 1 (gray). All results were obtained without  $Ca^{2+}$ .  $n = 13$ –16, depending on the voltage. The wild-type results are from Hoshi et al. (2013. *Proc. Natl. Acad. Sci. USA*. 110:4816–4821).